

Structure, Stereochemistry, and Biological Activity of Integramycin, a Novel Hexacyclic Natural Product Produced by *Actinoplanes* sp. that Inhibits HIV-1 Integrase

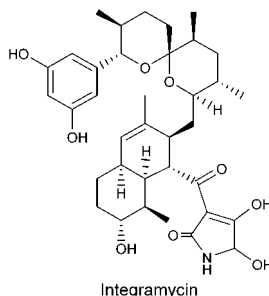
Sheo B. Singh,^{*,†} Deborah L. Zink,[†] Brian Heimbach,[†] Olga Genilloud,[‡] Ana Teran,[‡] Keith C. Silverman,[†] Russell B. Lingham,[†] Peter Felock,[§] and Daria J. Hazuda[§]

Merck Research Laboratories, Rahway, New Jersey 07065, and West Point, Pennsylvania 19486, and Centro de Investigación Básica, Laboratorios Merck Sharp & Dohme de Espana, S. A. Josefa Valcárcel 38, 28027 Madrid, Spain

sheo_singh@merck.com

Received January 10, 2002

ABSTRACT



HIV-1 integrase is a critical enzyme for viral replication, and its inhibition is an emerging target for potential antiviral chemotherapy. We have discovered a novel inhibitor, integramycin, from screening of fermentation extracts using an in vitro assay. Integramycin possesses a hexacyclic ring system and exhibited an IC_{50} value of $4 \mu M$ against HIV-1 integrase (strand transfer). The isolation, structure elucidation, stereochemistry, conformation, and biological activity has been described.

HIV-1 integrase is a critical enzyme responsible for the integration of the HIV genome into the host genome. Integration is a three-step process that includes assembly of proviral DNA on integrase, endonucleolytic processing of the proviral DNA, and strand transfer of the proviral DNA into the host cell DNA.¹ This is a unique event by which

the virus propagates and is absent from the host and, therefore, presents a safe target for development of anti-HIV therapy used either alone or in combination with existing (protease and reverse transcriptase inhibitor) therapies. Recently, we reported diketo acid (DKA) based inhibitors of integrase, which were almost as potent as HIV-1 protease inhibitors in antiviral assays and validated that inhibition of integrase potentially blocks replication of HIV-1 in whole cells.²

* To whom correspondence should be addressed at Merck Research Laboratories, RY80Y-355, P.O. Box 2000, Rahway, NJ 07065. Fax: (732) 594-6880.

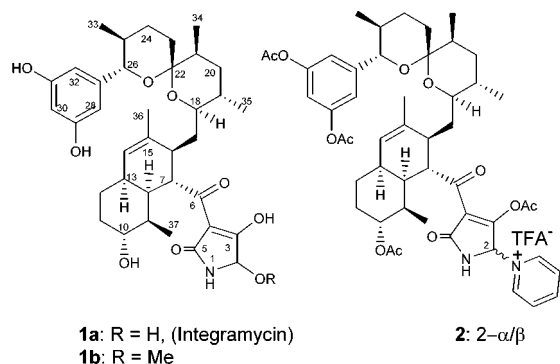
[†] MRL, Rahway.

[‡] CIBE, Spain.

[§] MRL, West Point.

(1) For recent reviews on HIV integrase, see: (a) Craigie, R. *J. Biol. Chem.* **2001**, *276*, 23213. (b) Esposito, D.; Craigie, R. *Adv. Virus Res.* **1999**, *52*, 319.

Even though DKA's are valid small-molecule leads that could potentially be refined into clinical agents, alternative lead structures are urgently needed.



Natural product extracts have been successful in providing novel leads for many biological targets. Screening of such extracts against recombinant HIV-1 integrase led to the discovery of several natural product inhibitors, including equisetin,³ integric acid,⁴ and complestatin.⁵ Continued screening of *Actinoplanes* extracts led to the discovery of integramycin (**1a**), a novel hexacyclic natural product that inhibited recombinant HIV-1 integrase strand transfer reaction with an IC₅₀ value of 4 μ M. The isolation, structure, stereochemistry, conformation, and biological activities of integramycin (**1a**) and derivatives are herein described.

Size exclusion (Sephadex LH 20) chromatography of a methyl ethyl ketone extract of *Actinoplanes* sp. (ATCC202188), grown on a liquid media, followed by reversed-phase HPLC on a Zorbax RX C-8 column afforded integramycin (200 mg/L) as a colorless powder, $[\alpha]_D^{23} = +30.6$ (*c* 2.35, MeOH).

High-resolution ESIMS analysis of integramycin provided a molecular formula of C₃₆H₄₉NO₉ + NH₄ (found 657.3752, calcd 657.3745), which was corroborated by ¹³C NMR spectra of **1a** in C₅D₅N and acetone-*d*₆ (Table 1). ¹³C NMR spectra revealed the presence of five methyls, six methylenes, 16 methines, including four olefinic/aromatic and two oxymethines, a bis-oxy quaternary carbon, and two olefinic quaternary, two meta-substituted dihydroxy aromatic, and three ketone-type carbons. The UV spectrum of **1a** showed absorption bands at λ_{\max} 209 ($\epsilon = 20\ 685$), 250 (5770), and 284 (12 410) nm. The IR spectrum exhibited absorption

bands for hydroxy (ν_{\max} 3275 cm⁻¹), conjugated ketones (ν_{\max} 1656 cm⁻¹), and aromatic (ν_{\max} 1594 cm⁻¹) groups. The ¹H NMR spectrum of integramycin displayed a complex pattern with overlapping signals and exhibited tautomeric equilibria, resulting in new NMR signals after only a brief exposure to various solvents. Elucidation of the structure therefore required data collection in several solvents. C₅D₅N and acetone-*d*₆ provided superior signal dispersion in the ¹H NMR spectrum despite tautomeric equilibration that was significantly pronounced in the latter solvent. The ¹H-¹H spin systems were discerned by 2D COSY and 2D TOCSY spectra. The combination of the two methods together with 1D TOCSY data revealed the presence of three contiguous spin systems: (a) H14-H13-(H8)-H12-H11-H10-H9-(H37)-H8-H7-H16-H17-H18-H19-(H35)-H20-H21-H34, (b) H26-H25-(H33)-H24-H23, and (c) H28-(H32)-H30. These fragments were further verified by HMQC and HMBC ($^nJ_{\text{XH}} = 7$ and 5 Hz) experiments in both solvents. In particular, the strong HMBC correlations from five methyl groups were extremely valuable in the final elucidation of the structure of **1a**. Selected HMBC correlations are listed in Table 1. The olefinic methyl group (H₃-36, δ 1.83) showed three strong HMBC correlations to the C-14 (δ 127.6), C-15 (δ 136.4), and C-16 (δ 40.8), thus linking C-14 to C-16 via C-15. The HMBC correlations from H-16 to C-6, C-8, C-14, C-15, and C-18 allowed the confirmation of a segment of fragment A and allowed the extension of fragment A to the C-6 keto group. Correlations of C-34 and C-35 methyl groups to C-20 and C-21 and C-18, C-19 and C-20, respectively, further confirmed the fragment A assignments. In addition, the H₃-34 produced an HMBC correlation to the C-22 bis-oxy carbon (δ 98.7), which also showed an HMBC correlation to H-26 (only in acetone-*d*₆ with $^nJ_{\text{XH}} = 5$ Hz). Additionally, H-26 showed numerous expected HMBC correlations (Table 1), including correlations to aromatic carbons C-27 and C-28, thus establishing the linkage of fragments A to B and the aromatic unit C. The C-3 OH (δ 8.26) showed HMBC correlations (acetone-*d*₆, $^nJ_{\text{XH}} = 5$ Hz) to C-2, C-3, and C-4, thus confirming the enolic tautomer of the tetramic acid unit as shown, which is in part similar to the tetramic acid unit of equisetin and phomasetin.⁴ The apparent one-bond HMBC correlations of the two aromatic proton doublet (δ 7.04 \rightarrow 107.4) indicated the symmetric nature of the aromatic ring. The highly deshielded ¹H NMR shift of H-7 (δ 4.36 in C₅D₅N and δ 3.83 in acetone-*d*₆) is noteworthy and probably caused by the anisotropic effect due to the facial proximity of the dihydro-pyrrolidone ring. Protons present near the polarizing oxygen experienced significant shifts in the ¹H NMR spectrum recorded in C₅D₅N when compared with corresponding proton signals in the acetone-*d*₆ spectrum (Table 1). The EIMS analysis of the hexasilyl ether produced corrected fragment ions at *m/z* 479.3155 (calcd for C₃₁H₄₃O₄, 479.3163), *m/z* 142.0155 (calcd for C₅H₄NO₄, 142.0140), *m/z* 305.1751 (calcd for C₁₈H₂₅O₄, 305.1754), and *m/z* 461.2772 (calcd for C₂₆H₃₉NO₆, 461.2779) due to cleavages of C6-C7, C17-18, C22-oxygen, and C24-25 bonds, respectively (Figure 1), further confirming the structural assignment.

(2) (a) Hazuda, D. J.; Felock, P.; Witmar, M.; Wolfe, A.; Stillmock, K.; Grobler, J. A.; Espeseth, A.; Gabrylski, L.; Schleif, W.; Blau, C.; Miller, M. D. *Science* **2000**, *287*, 646. (b) Wai, J. S.; Egbertson, M. S.; Payne, L. S.; Fisher, T. E.; Embrey, M. W.; Tran, L. O.; Melamed, J. Y.; Langford, H. M.; Guare, J. P.; Zhuang, L.; Grey, V. E.; Vacca, J. P.; Holloway, M. K.; Naylor-Olsen, A. M.; Hazuda, D. J.; Felock, P. J.; Wolfe, A. L.; Stillman, K. A.; Schleif, W.; Gabrylski, L. J.; Young, S. D. *J. Med. Chem.* **2000**, *43*, 4923. (c) Neamati, N. *Exp. Opin. Invest. Drugs* **2001**, *10*, 281.

(3) Singh, S. B.; Zink, D. L.; Goetz, M. A.; Dombrowski, A. W.; Polishook, J. D.; Hazuda, D. L. *Tetrahedron Lett.* **1998**, *39*, 2243.

(4) (a) Singh, S. B.; Zink, D. L.; Polishook, J.; Valentino, D.; Shafiee, A.; Silverman, K.; Felock, P.; Teran, A.; Vilella, D.; Hazuda, D. J.; Lingham, R. B. *Tetrahedron Lett.* **1999**, *40*, 8775. (b) Singh, S. B.; Felock, P.; Hazuda, D. J. *Bioorg. Med. Chem. Lett.* **2000**, *10*, 235.

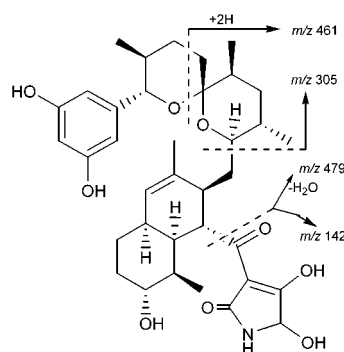
(5) Singh, S. B.; Jayasuriya, H.; Salituro, G. M.; Zink, D. L.; Shafiee, A.; Heimbuch, B.; Silverman, K. C.; Lingham, R. B.; Genilloud, O.; Teran, A.; Vilella, D.; Felock, P.; Hazuda, D. *J. Nat. Prod.* **2001**, *64*, 874.

Table 1. ^1H and ^{13}C NMR Assignment of Integramycin (**1a**) in $\text{C}_5\text{D}_5\text{N}$ and Acetone- d_6 ^a

position	δ_{C}	type	$\text{C}_5\text{D}_5\text{N}$		HMBC (H \rightarrow C), ⁿ $J_{\text{XH}} = 7$ Hz	acetone- d_6	
			δ_{H}			δ_{C}	δ_{H}
2	81.8	CH	5.84, br s			81.1	5.12, s
3	196.3	C $^\circ$		H-2		194.3	
4	103.3	C $^\circ$				102.6	
5	177.1	C $^\circ$		H-2		176.4	
6	192.3	C $^\circ$		H-7, H-16		192.2	
7	43.3	CH	4.36, dd, 12.5, 9.6			42.9	3.83, dd, 12.5, 9.5
8	42.7	CH	2.58, td, 4, 12.5	H-14, H-16, H-37		43.0	2.36, td, 4, 12.5
9	46.2	CH	1.95, m	H-37		45.9	1.65, m
10	70.6	CH	4.24, dt, 4, 10	H-37		70.7	3.51, dt, 4.5, 12.5
11	37.8	CH ₂	2.31e, m; 1.60a, m			37.2	1.95, m; 1.30, m
12	30.4	CH ₂	1.75e, m; 1.50a, m			30.2	1.70, m; 1.35, m
13	39.8	CH	2.10, m	H-7, H-14		39.9	2.1, m
14	127.6	CH	5.50, brd, 6	H-16, H-36		127.5	5.53, dt, 6.5, 1.5
15	136.4	C $^\circ$		H-16, H-36		136.6	--
16	40.8	CH	3.07, dt, 1.5, 9	H-7, H-14, H-36		40.8	2.71, br t, 8
17	40.0	CH ₂	1.95 α , br dd, 9, 13; 1.85 β , br dd, 10, 13			39.8	1.75, m; 1.45, m
18	74.5	CH	3.50, t, 10	H-16, H-35		74.5	3.22, ddd, 1.6, 10.5, 11.5
19	30.9	CH	1.29, m	H-35		30.9	1.20, m
20	35.4	CH ₂	1.98, m; 1.05, m	H-34, H-35		35.6	1.75, m; 1.14, ddd, 2.5, 4.5, 13
21	37.2	CH	1.75, m	H-34		37.3	1.65, m
22	98.7	C $^\circ$		H-20, H-26, H-34		98.7	
23	33.9	CH ₂	2.05e, m; 1.39a, m			33.9	1.70, m; 1.3, m
24	29.3	CH ₂	2.05e, m; 1.70a, m	H-26, H-33		29.2	
25	37.2	CH	1.75, m	H-34		37.2	1.49, m
26	80.1	CH	4.41, d, 10	H-28, H-33		79.8	3.97, d, 10
27	145.6	C $^\circ$		H-26		145.2	
28	107.4	CH	7.04, d, 2	H-26, H-30, H-32		107.0	6.36, d, 2.5
29	160.4	C $^\circ$		H-28, H-30		159.1	
30	103.6	CH	6.94, t, 2	H-28		102.6	6.27, t, 2
31	160.4	C $^\circ$		H-30, H-32		159.1	
32	107.4	CH	7.04, d, 2	H-26, H-28, H-30		107.0	6.36, d, 2.5
33	18.8	CH ₃	0.89, d, 6.4	H-26		18.5	0.68, d, 7.0
34	15.5	CH ₃	0.95, d, 7.2			15.3	0.87, d, 7.0
35	18.4	CH ₃	0.56, d, 6.4			18.5	0.68, d, 7.0
36	23.0	CH ₃	1.83, d, 1.5			22.7	1.74, br s
37	17.5	CH ₃	1.38, d, 7.2			16.8	1.03, d, 7.0
C-3 OH			10.8, br s				8.26, s

^a e = equatorial, a = axial; the magnitude of the J values of H-17 were determined from 1D TOCSY experiment.

Integramycin (**1a**) reacted with methanol to produce a C-2 epimeric mixture of the methoxy ether **1b** [FABMS m/z 654 (M + H)⁺; ^1H NMR (acetone- d_6) δ 5.00 (s, H-2), 86.6 (C-

**Figure 1.** EIMS fragmentation of integramycin (**1a**).

2), 3.38 (s, OMe)]. Acetylation of **1a** with acetic anhydride in pyridine produced a chromatographically separable 1:1 mixture of C-2 epimeric pyridinium tetraacetates **2** [FABMS, m/z 869.4223 (M + H)⁺, C₄₉H₆₁N₂O₁₂]. The H-2 (δ 6.06, s) of **2** showed strong HMBC (CD₃CN) correlations to C-5 (δ 172.2), C-3 (δ 181.6), and C-2' (δ 141.4) of pyridine, thus proving the evidence of the attachment of the pyridine nitrogen at C-2. These derivatives provide further structural confirmation of the heterocyclic unit of **1a**.

Stereochemistry. The relative stereochemistry of integramycin (**1a**) was deduced by a combination of vicinal couplings, NOESY correlations, ChemDraw three-dimensional modeling, and examination of Dreiding models. H-7 of the Decalin system displayed large couplings with H-8 ($J_{\text{H}7,8} = 12.5$ Hz) and H-16 ($J_{\text{H}7,16} = 9.6$ Hz), indicating a diaxial relationship of these protons, which was supported by NOESY correlations of H-8 and H-16 (Figure 1). H-8 showed identical 4 Hz couplings with both H-9 and H-13,

suggesting axial geometries of these protons in the cyclohexyl ring (H-8 becomes equatorial with respect to H-9 and H-13) in a cis-fused Decalin system. Here, the chair cyclohexyl ring sits perpendicularly to the cyclohexene ring, which adapts a half-chair conformation. Likewise, H-10 showed two large couplings (both $J = 10$ Hz) with H-9 and axial H-11, indicating the axial disposition of H-10. These stereochemical assignments were confirmed by NOESY correlations of H-8 with H-13, H-9, and H₃-37. Similarly, H-26 of the spiro-bis-pyran system showed a large coupling with H-25 ($J = 10$ Hz), indicating diaxial geometries of H-25 and H-26, thus establishing the equatorial orientations of the dihydroxy phenyl and methyl groups at C-26 and C-25, respectively. The other oxymethine H-18 of the spiro-bis-pyran system displayed a large coupling ($J = 10$ Hz) with H-19 due to axial-axial interactions and showed a large coupling ($J = 10$ Hz) with only one of the C-17 methylene protons (δ 1.85, β H), indicating an anti relationship of the two protons. Similarly, the second C-17 methylene proton (δ 1.98, α H) showed a large coupling ($J = 9$ Hz) with H-16 due to their anti relationships. Except for the geminal coupling, these methylene protons did not exhibit any other observable couplings. The ChemDraw three-dimensional model (Figure 2) of **1a** suggested dihedral angles of 170–180° between the vicinal coupling partners (H-16 and H-17 α ; H-18 and H-17 β) and 80–85° between the vicinal non-coupling partners, confirming the observed J values between the corresponding protons (see Figure 3 in Supporting Information for a relaxed stereo version of Figure 2). The H-19 gave NOESY correlations to H₃-21, thus confirming the axial geometry of the methyl group at C-21, which was further supported by the NOESY correlation of the methyl group with equatorial H-23 (δ 2.05). H-18 showed strong NOESY correlations to H-26, suggesting a cup-shaped conformation of the spiro-bis-pyran system. Both H-18 and H-26 showed NOESY correlations to H-16 and H₃-36, indicating that they were at the same plane and thus relaying the stereochemistries of the Decalin unit with the spiro-bis-pyran unit connected through the C-17 methylene group. This assignment was further supported by a NOESY correlation of H₃-35 with H-17 β (δ 1.85) and ChemDraw three-dimensional and Dreiding models. The relative stereochemistry (7*S*,8*R*,9*R*,13*R*,16*S*,18*R*,19*S*,21*S*,23*R*,25*S*,26*S*) and solution conformation of integramycin (**1a**) are shown in Figure 2.

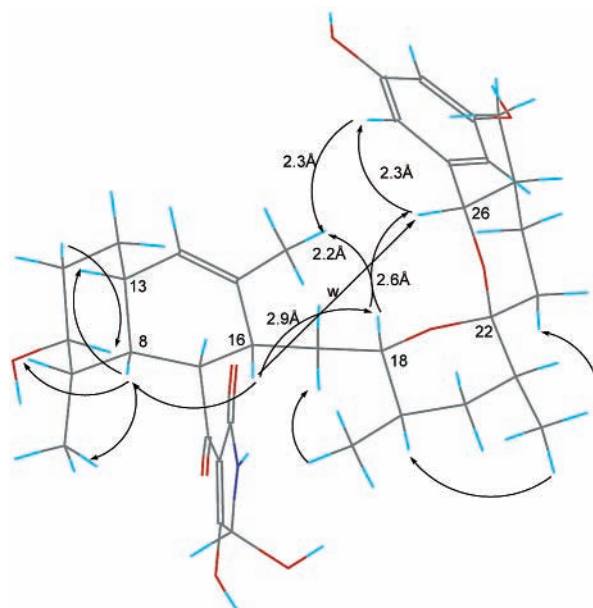


Figure 2. ChemDraw three-dimensional molecular model with selected NOESY correlations (mix = 700–1000 ms) of integramycin (**1a**) in C₃D₅N.

Integramycin (**1a**) inhibited HIV-1 integrase coupled and strand transfer reactions with IC₅₀ values of 3 and 4 μ M, respectively. The methyl ether (**1b**) displayed a comparable inhibition profile to **1a** and exhibited IC₅₀ values of 6.1 μ M in each of the two assays. Both epimeric pyridinium acetates (**2**) were as potent as **1b** in the coupled assay and showed IC₅₀ values of 6 μ M, but they were over 5-fold less active in strand transfer assays (IC₅₀ = 30–46 μ M). Integramycin was not active in DNase assay at 100 μ M.

In summary, we have described the discovery of integramycin, which is a complex natural product with significant and novel activity against HIV-1 integrase, a target for new anti-HIV therapy.

Supporting Information Available: Copies of ¹H and ¹³C NMR spectra of **1a**, **1b**, and both epimers of **2**, a 1D TOCSY spectrum of **1a**, and a ChemDraw three-dimensional stereoview. This material is available free of charge via the Internet at <http://pubs.acs.org>.

OL025539B